In-situ Growth Observation of GaN/AlGaN Superlattice Structures by Simultaneous x-Ray Diffraction and Ellipsometry

C. Simbrunner[1], Tian Li[1], M. Wegscheider[1], A. Navarro-Quezada[1], M. Quast[1], A. Bonanni[1], A. Kharchenko[2], J. Bethke[2], K. Lischka[3], H. Sitter[1]

[1] Institut für Halbleiter- und Festkörperphysik, Johannes-Kepler-Universität Linz, A-4040 Linz

[2] PANalytical B.V., Almelo, The Netherlands

[3] Department of Physics, University of Paderborn, Germany

A considerable effort has been lately invested in the improvement of optical-based *in-situ* methods for the real-time control of metallorganic chemical vapor deposition (MOCVD) processes. In this report we present a novel approach combining *in-situ* x-ray diffraction and spectroscopic ellipsometry applied during the MOCVD of GaN/AlGAN superlattices.

Introduction

During the last years III-nitride semiconductors established for the production of opto- and high power electronic devices [1]. The optimization of superlattice structures (SL) is the key to increase the efficiency of several devices, *e.g.* nitride based vertical cavity surface emitting lasers. Furthermore, low dimensional structures improve the electrical properties of semiconducting materials [2]. Metal organic chemical vapor deposition (MOCVD) of epitaxial layers works at non-ultra high vacuum conditions and consequently electron based methods like reflection high energy electron diffraction are excluded from the possible spectrum of *in-situ* characterization techniques, narrowing the window to optical based ones like spectroscopic ellipsometry (SE) [3], [4], laser reflectometry [5], [6] and in-situ x-ray diffraction (IXRD) [7], [8]. Recently, complementary techniques have been combined, leading to consistent and extended information, as it was shown for SE combined with laser reflectometry [9] and micromechanical cantilever-based sensing [10]. In this article we focus on the *in-situ* and on-line monitoring of the MOCVD of GaN/AlGaN superlattice structures, accomplished through a novel approach based on the simultaneous use of SE and IXRD. The combination of surface- and bulk-sensitivity yields complementary and consistent information on the growing layers.

Experimental Procedure

All experiments were performed in an AIXTRON 200 RF-S horizontal flow reactor whose geometry allows simultaneous SE and IXRD *in-situ* measurements. Further details on the IXRD setup and data acquisition can be found elsewhere [11], [12]. Two optical windows allow *in-situ* SE in the energy range 1.5 – 5.5 eV. By applying the common pseudosubstrate approximation (CPA) to kinetic ellipsometry data layer-thickness, -composition and growth rate can be determined [9], [13]. For epitaxial layers, a complex pseudo-dielectric function $\langle\varepsilon_p\rangle$, summarizing the whole sample structure, can be

obtained [13] and consists of an imaginary ε_i and a real ε_r part. In the case of an optically thick material, ε_r considered as a function of ε_i, generates in the complex plane logarithmic spirals, whose converging points represent the dielectric function of the growing layer at the given energy and temperature. Therefore, by choosing the ellipsometer wavelength above the energy gap of the growing material and by applying the CPA, $\langle\varepsilon_p\rangle$ and consequently the composition and growth rate of the growing layer can be determined in real time.

All samples have been fabricated using trimethylgallium (TMGa), trimethylaluminum (TMAl) and ammonia as precursors. Upon deposition of a low temperature GaN nucleation layer on the (0001) sapphire substrate, a GaN buffer layer of 1 µm was deposited using standard procedures [9]. In order to prove the complementarity of the two techniques, a 500 nm thick AlGaN layer was grown onto the GaN buffer and kinetic ellipsometry measurements at photon energy of 3.815 eV have been performed. The resulting values for ε_i are reported in Fig. 1(a) as a function of time. Fig. 1(b) outlines the acquired SE data in the complex plane by plotting ε_r as a function ε_i. By applying the CPA, data points have been fitted and are indicated by solid lines in the plots. The increasing time scale is indicated by arrows. Simultaneously measured IXRD spectra are given in Fig. 1(c) as a contour plot illustrating the spectral intensity as a function of time and of the detection angle Δε relative to GaN buffer peak. The time scale is taken relative to the start of the SL structure, grown onto the AlGaN intermediate layer, and has been synchronized for IXRD and SE measurements.

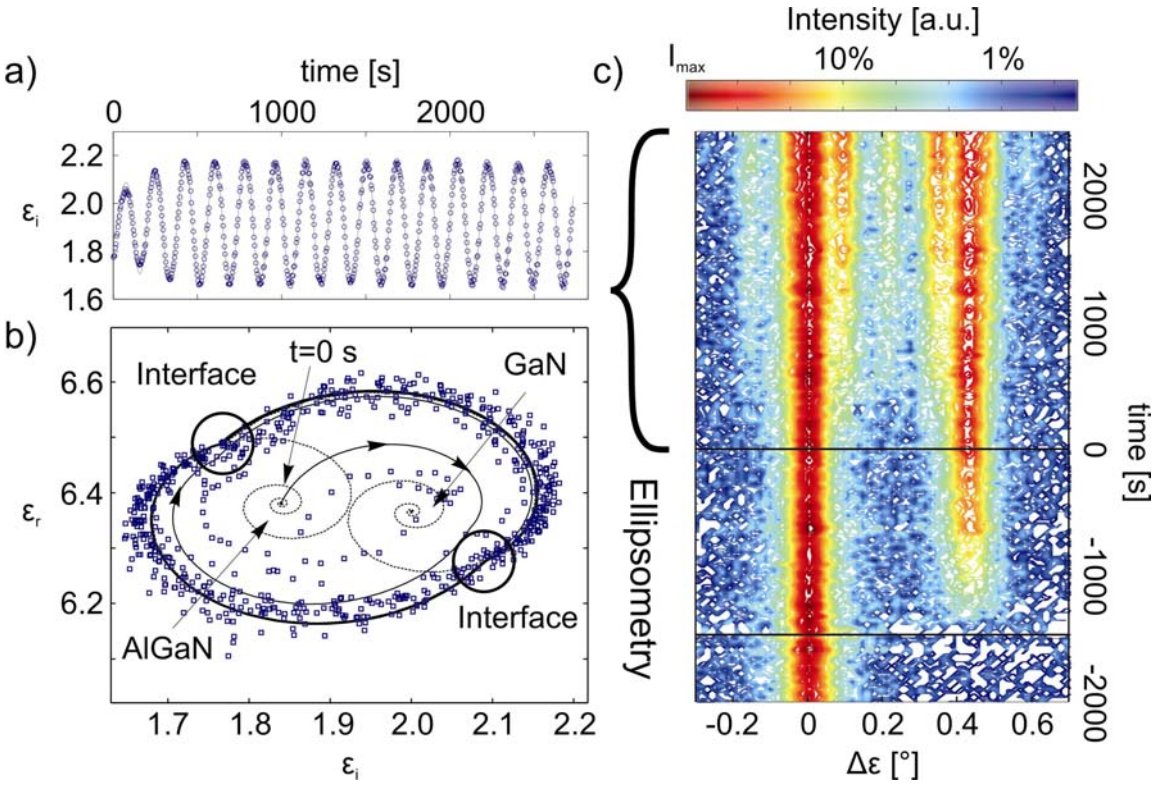

Fig. 1: (a) ε_i as a function of time. (b) ε_r as a function of ε_i acquired by SE during SL growth (blue rectangles). Solid lines represent the fit to the data. (c) Contour plot of IXRD spectra acquired simultaneously during GaN buffer, AlGaN and SL growth as a function of time and diffraction angle Δε relative to GaN buffer peak.

With the increase of the AlGaN layer thickness and due to the constant alloy composition, the value of ε_r as a function of ε_i converges on the complex plane. At t = 0 s the value corresponds to the pseudo-dielectric function of a growing layer with a well defined Al content. SE measured in the absorbing region of the growing compound ceases to provide information as soon as the layer becomes optically thick. On the other hand, at this thickness the layer is still transparent to the x-rays and a peak originating from the GaN buffer situated 500 nm below the surface is detectable. More detailed studies of the growing AlGaN layers show a dynamic behavior of the integrated peak intensity which increases linear with the layer thickness [7] and can be assigned to the increasing number of lattice planes contributing to the diffracted signal. By turning off the TMAl source at t = 0 s the deposition of the SL is accomplished by periodically switching the TMAl source every 90 s. As an effect of the change to GaN growth $\varepsilon_i(\varepsilon_r)$ follows a different logarithmic spiral converging at the center of the GaN helix, as shown in Fig. 1(b). The oscillations of ε_i as a function of time reported in Fig. 1(a) result from the periodic change of the growth conditions generating a competing behavior between GaN and AlGaN spirals. After 2 – 3 grown SL periods the SE response is balanced and results in two spiral tails in the complex plane indicated by solid lines in Fig. 1(b). Interfaces in the grown SL structure are characterized by discontinuity points of the spirals and underline the sensitivity of SE to surface effects.

The fitted SL periodicity and layer composition determined by SE are listed in Tab. I indicated by footnotes. The calculations are based on calibration curves relating the Al concentration to the corresponding dielectric function [9]. In contrast to the surface sensitive and fast responding SE, the SL peaks become visible in IXRD after 2 – 3 grown periods. By choosing for the SL the same Al concentration as for the AlGaN intermediate layer and with an identical period thickness for the GaN and AlGaN layers, the SL-0 peak is centered between the GaN buffer and the AlGaN intermediate layer peaks. By fitting the IXRD spectra the SL periodicity and concentration can be evaluated. The detected peak positions determine the achieved Al concentration by applying the Vegard's law and the periodicity can be easily deduced from the distances between the single SL peaks. The resulting values for GaN and AlGaN layer thickness and Al concentrations are listed in tab. I and are in excellent agreement with the values originating from SE measurements.

	d_{GaN} [nm]	d_{AlGaN} [nm[	Al conc.
AlGaN	-	-	15.02% (15.49%[a])
SL	36.07 (36.96[a])	36.29 (36.89[a])	14.05% (15.49%[a])

Tab. I: Fitted IXRD SL layer thickness and composition compared with values obtained by SE indicated by the footnote.

References

[1] O. Ambacher, J. Phys. D: Appl. Phys. **31**, 2653 (1998)

[2] A. Y. Polyakov, et. al., Appl. Phys. Lett. **79**, 4372 (2001)

[3] A. Bonanni, et. al., J. Cryst. Growth **275**, e1763 (2005)

[4] M. Drago, P. Vogt and W. Richter, phys. stat. sol. (a) **203**, 116 (2006)

[5] N. Dietz, Mat. Sci. Eng. B **87**, 1 (2001)

[6] B. Beaumont, et. al., J. Cryst. Growth **170**, 316 (1997)

[7] C. Simbrunner, et. al., phys. stat. sol. (a) **203**, 1704 (2006)

[8] P. Fuoss, et. al., Phys. Rev. Lett. **69**, 2791 (1992)

[9] A. Bonanni, et. al., J. Cryst. Growth **248**, 211 (2003)

[10] M. Godin, et. al., Rev. Sci. Instr. **74**, 4902 (2003)

[11] C. Simbrunner, et. al., J. Cryst. Growth **298**, 243 (2007)

[12] A. Kharchenko, et. al., Rev. Sci. Instr. **76**, 033101 (2005)

[13] D. E. Aspnes and N. Dietz, Appl. Surf. Sci. **130-132**, 367 (1998)